DESIGN, CONSTRUCTION AND FACILITY ENHANCEMENT FOR DIGITAL NEUTRON RADIOGRAPHY AT REACTOR TRIGA PUSPATI

MUHAMMAD SYAHIR BIN SARKAWI

A thesis submitted in fulfilment of the
requirements for the award of the degree of
Doctor of Philosophy

School of Chemical and Energy Engineering
Faculty of Engineering
Universiti Teknologi Malaysia

JANUARY 2020

ACKNOWLEDGEMENT

"In the name of Allah, the Most Gracious and the Most Merciful."

First and foremost, a special thank you to my supervisor, Dr. Jasman Zainal, for all his guidance, support, advice, and providing time to discuss my work. He has taught me more than I could ever give him credit for here. I also would like to acknowledge my co-supervisor, Dr. Faridah Idris from the Malaysian Nuclear Agency (MNA) for all her suggestions, time, and help throughout my research.

I would also like to express my sincere gratitude to MNA for providing the research facility and their staffs Dr. Muhammad Rawi, Mrs. Khair'iah Yazid, Mr. Hairie Rabir and Mr. Rafhayudi Jamro who have given me valuable opportunity to have used of their resources, equipment, and for all their assistance.

This work would not have been possible without financial support from Universiti Teknologi Malaysia (UTM), and Ministry of Education Malaysia under *Skim Latihan Akademik Muda* (SLAM).

Nobody has been more important to me in the pursuit of this research than the members of my family and friends. I would like to thank my parents, who support me from the beginning of my journey. They are the ultimate role models. Most importantly, I am grateful to my loving and supportive wife, Najaa Fadhilah, who provide continual inspiration.

ABSTRACT

Neutron radiography (NR) is an important application in non-destructive testing which has been used especially in industrial, nuclear material, medical and agriculture. Reactor TRIGA PUSPATI (RTP) is the only research reactor in Malaysia which located at the Malaysian Nuclear Agency, with total capacity of 1MW operation. Its main applications are neutron activation analysis, small angle neutron scattering, and neutron radiography. The first NR facility system in RTP was ready for use in 1985. However, this neutron radiography facility known as NUR-2 was disassembled in 2014 due to several factors such as low collimation ratio, low thermal neutron flux, high gamma dose, and inadequate radiation shielding. Thus, there is a need to upgrade the capabilities of existing neutron radiography facility to meet current users' needs. Monte Carlo simulation code of MCNPX was used to simulate the important parameters and instrument design of the new neutron radiography facility. This simulation code of the neutron beam helps to design experiments before placing any sample objects in the neutron beam. The new collimator, beam shutter, and shielding were fabricated based on the results from Monte Carlo simulations while the concrete mixture of the new exposure room shielding was formulated using Department of Environmental's design method. The concrete samples were tested in terms of radiation shielding capability and strength. The best mix design was chosen to be fabricated as new exposure room shielding for NR facility at RTP. Furthermore, results obtained from the experimental works were used to verify the simulation modelling. Based on the simulation results, the new NR facility has a thermal neutron flux of 3.86×10^3 $\mathrm{ncm^{-2}s^{-1}}$ at the sample position. The new collimated beam has been characterized using beam purity indicator and sensitivity indicator from American Society for Testing and Materials. Radiographs of a sensitivity indicator taken using both digital and conventional direct film radiographic method provide one example of the radiographic capabilities of the new facility. The neutron radiograph which was taken by charged-coupled device camera and film showed that digital neutron radiography is not currently capable of producing good quality radiographs but it is mainly due to the limitations of the digital detector itself.

ABSTRAK

Radiografi neutron (NR) merupakan satu aplikasi yang penting telah digunakan dalam ujian tanpa musnah terutama sekali dalam bidang industri, bahan nuklear, perubatan, dan pertanian. Reaktor TRIGA PUSPATI (RTP) merupakan satu-satunya reaktor penyelidikan di Malaysia yang terletak di Agensi Nuklear Malaysia (ANM) dan dengan jumlah kapasiti pada 1 MW operasi. Aplikasi utama di reaktor ini adalah analisis pengaktifan neutron, serakan neutron sudut kecil, dan radiografi neutron. Sistem kemudahan NR yang pertama di RTP telah mula digunakan pada tahun 1985. Namun, kemudahan radiografi neutron ini yang dikenali sebagai NUR-2 telah ditutup pada tahun 2014 disebabkan oleh beberapa faktor seperti nisbah pengkolimat yang rendah, fluks neutron terma yang rendah, dos gama yang tinggi, dan pemerisaian sinaran yang tidak mencukupi. Oleh itu, menaik taraf keupayaan kemudahan radiografi neutron sedia ada adalah sangat penting bagi memenuhi keperluan pengguna masakini. Perisian simulasi Monte Carlo MCNPX digunakan untuk mensimulasikan parameter penting dan reka bentuk instrumen kemudahan radiografi neutron yang baharu. Kod simulasi alur neutron ini membantu dalam merekabentuk eksperimen sebelum meletakkan sebarang sampel dalam alur neutron. Pengkolimat baharu, penutup alur, dan perisai sinaran direka berdasarkan keputusan dari simulasi Monte Carlo manakala campuran konkrit perisai bilik pendedahan baharu direkabentuk menggunakan kaedah yang diperolehi dari Jabatan Alam Sekitar. Sampel konkrit telah diuji dari segi pemerisaian sinaran dan ketahanan. Campuran konkrit terbaik dipilih untuk dijadikan sebagai pemerisaian bilik pendedahan yang baharu untuk kemudahan NR di RTP. Selain itu, keputusan yang diperoleh daripada kerja eksperimen digunakan untuk mengesahkan pemodelan simulasi. Berdasarkan keputusan simulasi, kemudahan NR baharu mempunyai fluks neutron terma sebanyak $3.86 \times 10^3\ \mathrm{ncm^{-2}s^{-1}}$ pada kedudukan sampel. Alur pengkolimat baharu telah dicirikan dengan menggunakan penunjuk alur ketulenan dan penunjuk kepekaan dari persatuan Amerika untuk pengujian dan bahan. Radiograf penunjuk kepekaan yang diambil menggunakan kedua-dua kaedah digital dan kebiasaan langsung radiografi filem menunjukkan satu contoh keupayaan kemudahan radiografi neutron baharu. Radiografi neutron yang diambil oleh kamera peranti cas terganding dan filem menunjukkan radiografi neutron secara digital tidak mampu menghasilkan radiograf yang berkualiti disebabkan keterbatasan pengesan digital itu sendiri.

TABLE OF CONTENTS

LIST OF TABLES

LIST OF FIGURES

LIST OF ABBREVIATIONS

Al_2O_3	-	Aluminium Oxide
ALARA	-	As Low As Reasonably Achievable
ASTM	-	American Society for Testing and Materials
BENSC	-	Berlin Neutron Scattering Centre
BNCT	-	Boron Neutron Capture Therapy
BPE	-	Borated Polyethylene
BPI	-	Beam Purity Indicator
CCD	-	Charged-Coupled Device
DOE	-	Department of Environmental, United Kingdom
EPDM	-	Ethylene Propylene Diene Monomer
FRM-II	-	Forshungsreaktor Munchen II
GADOX	-	Gadolinium Oxysulfide
GM	-	Geiger Muller
HFIR	-	High Flux Isotope Reactor
HFR	-	High Flux Reactor
IQI	-	Image Quality Indicator
JRR-3M	-	Japan Research Reactor-No.3 Modified
MCNP	-	Monte Carlo Neutron Particle
MCNPX	-	Monte Carlo Neutron Particle version X
MNA	-	Malaysian Nuclear Agency
NAA	-	Neutron Activation Analysis
NBSR	-	Neutron Beam Split-Core Reactor
NDT	-	Non-Destructive Testing
NR	-	Neutron Radiography
NRU	-	National Research Universal reactor
OPAL	-	Open Pool Australian Lightwater reactor
PGNAA	-	Prompt Gamma Neutron Activation Analysis
PPE	-	Personal Protective Equipment
RTP	-	Reactor TRIGA PUSPATI
SANS	-	Small Angle Neutron Scattering

SI	-	Sensitivity Indicator
TLD	-	Thermoluminescent Dosimeter
UTM	-	Universiti Teknologi Malaysia

LIST OF SYMBOLS

A	-	activity [Bq]
α	-	alpha particle
A	-	area
β	-	beta particle
R_{cd}	-	Cadmium Ratio
λ	-	decay constant [s^{-1}]
ρ	-	density [g/cm^3]
D	-	diameter
eV	-	electronvolt
σ_{epi}	-	Epithermal cross section
ϕ_{epi}	-	Epithermal flux [$cm^{-2}s^{-1}$]
γ	-	gamma-ray
g	-	gram
I_o	-	Incident neutron
Φ_o	-	Initial flux [$cm^{-2}s^{-1}$]
kg	-	kilogram
L	-	length [cm]
μ	-	linear attenuation coefficients [cm^{-1}]
n	-	neutron particle
σ	-	Neutron cross section [barn]
nv	-	Neutron flux per square centimetre per second
N	-	Number of target nuclides [$atoms/cm^3$]
R	-	Reaction rate
s	-	second
Sv	-	sievert
ϕ_{th}	-	Thermal flux [$cm^{-2}s^{-1}$]
σ_{th}	-	Thermal neutron cross section [barn]
t	-	thickness [cm]
μ_m	-	Total mass attenuation coefficients [cm^2/g]
I	-	Transmitted neutron

LIST OF APPENDICES

CHAPTER 1

INTRODUCTION

1.1 Overview

Neutron was discovered by an English physicist, Sir James Chadwick in 1932. Neutron is a particle that binds together with protons in the atomic nucleus. A neutron is neutrally charged and has a mass of about 1 amu, which is nearly the same with a proton (Davis, 2015). Different from X-ray and gamma-ray, neutrons interact with the nucleus of the atom rather than its electron cloud. Hence, the interaction force between neutrons and nuclei are not correlated with the atomic number of the element but instead depend on the isotope of the element (Anderson, McGreevy, & Bilheux, 2009). Neutrons have now been used for about 80 years to probe the microscopic structure and process in a complex matter.

Neutron imaging has been used more than seven decades since the first photograph capture by Kallman and Kuhn in Germany in 1935 (Kallmann, 1940). Since the mid-20th century, development of neutron imaging is ongoing showing that neutron is suitable for nondestructive testing in the study of bulk materials including aircraft components, fuel cell, cultural heritage, turbine blades, and biological samples (Fantidis, Potolias, & Bandekas, 2011; Rant, Milič, Turk, & Lengar, 2005; Satija, Jacobson, Arif, & Werner, 2004). Compared to X-ray and gamma-ray, the neutron has higher penetration power and could penetrate deeper into materials to give insight regarding the internal structures of these materials (Grupen, 2012).

As mentioned earlier, the concept of neutron radiography depends on the interaction of neutron with the target materials (Davis, 2015). The neutron transmitted through the target material could be captured as radiographic images by radiographic films or digitally by a charged-coupled device (CCD) camera (Azali Muhammad et

al., 2008). The amount of transmitted neutron is proportional to neutron scattering and neutron absorbing materials in the beam and can be determined using Beer's Law:

$$I = I_o \exp(-\mu \cdot t) \tag{1.1}$$

with, μ as the attenuation coefficients of the material, t as the thickness of the target sample, I_o as the intensity of the incoming neutron beam, and I as the intensity of the transmitted neutron through the target material.

There are three common neutron sources used for a variety of applications, which are nuclear reactors, accelerators, and radioisotopes(Domanus, 1992). In a research reactor, neutrons produced from the core are channeled through a beam port to the target sample, and the transmitted neutrons are used to gain insight into the internal structural properties of the sample object (Davis, 2015). Since neutron radiography is primarily performed with thermal neutrons, a collimator is needed to moderate the fast neutrons and filter gamma radiation (MacGillivray, 2011).

In Malaysia, the one and only research reactor is Reactor TRIGA PUSPATI (RTP) located at the Malaysian Nuclear Agency (MNA). Neutron beams from this reactor provide a good thermal neutron source for a variety of applications such as neutron activation analysis, isotope production, characterization of materials, and neutron radiography. In this research, several components of the previous neutron radiography facility will be redesigned in order to upgrade its capability. This research focuses on the main limitations of previous neutron radiography facility, which is low thermal neutron flux, high gamma radiation for digital neutron radiography, and inadequate radiation shielding. The newly upgraded neutron radiography facility will be evaluated using standard neutron radiographic sensitivity indicator and various sample objects (ASTM E545, 2014).

The types of concrete used in the new exposure room shielding can be grouped into two categories, namely grade-40 concrete, and high-density ferro boron concrete. According to the initial plan, all the concrete blocks were to be built using high density ferro boron concrete. However, due to budget limitation, the initial design has to be

modified in order to meet the financial terms and maintain the radiation shielding capability.

Monte Carlo simulation code of MCNPX is used to study various parameters that are needed to conduct neutron radiography testing at the beam port such as neutron and gamma flux and dose, design of collimator, and radiation shielding. The data and results obtained from simulations, experiments and real time neutron radiography practices on various types of objects will be compared and analyzed.

1.2 Problem Statement

RTP has a neutron radiography facility known as NUR-2 which has been used as a basic inspection tool since 1985 for archaeological and biological objects and industrial components. However, this facility has low thermal neutron intensity at the sample position, which leads to long irradiation times, and it gives many limitations for the industrial applications (Azali Muhammad et al., 2008). This facility also has low collimation ratio and high gamma radiation. Besides, its radiation shielding block is insufficient due to the streaming problem. The previous neutron radiography facility is only limited for the conventional radiographic method, which is using films due to high gamma radiation at the sample position area. Hence, due to this drawback NUR-2 was dissembled in 2014. Since then, neutron radiography can only be done at SANS (beam port 4) of RTP.

In this study, new neutron radiography facility instruments will be designed and constructed to upgrade previous outdated components. Many gaps which exist between the previous radiation shielding blocks at NUR-2 has led to the radiation streaming problem. Besides, the previous radiation shielding blocks were made from normal concrete. Thus, new radiation shielding blocks will be designed to reduce radiation streaming problem and ferro boron will be added into the concrete mixture to enhance its radiation shielding capability. Other than that, the previous beam shutter has a large dimension which is not suitable for the new neutron radiography facility.

Hence, a new beam shutter will be designed to be more compact and yet sufficient to block radiation coming from the beam port.

The charged coupled device (CCD) camera is used for capturing radiographic imaging of the samples. This device is more convenient to use than films in terms of image processing and analysis. However, using a CCD camera at the previous neutron radiography facility is quite impracticable and risky due to high radiation that can cause damage to the electronic parts inside the CCD camera. With new collimator and radiation shielding for the camera, this digital imaging at the new neutron radiography facility can be realized, and it will be a significant enhancement to the previous facility.

1.3 Research Objectives

The aim of this research is to upgrade the neutron radiography facility (NUR-2) for digital imaging at Reactor TRIGA PUSPATI, Malaysia. In an attempt to achieve this goal, the following tasks are established:

1. To improve collimator, beam shutter, and shielding bunker design
2. To fabricate the new radiation shielding block and beam shutter
3. To determine neutron and gamma profile
4. To demonstrate the new neutron radiography facility capabilities at RTP

1.4 Scope of the Study

This research aims to upgrade several parameters and the design of neutron radiography facility (NUR-2) at RTP. This research used thermal neutrons from the radial beam port (beam port 3) of RTP. New neutron radiography components at RTP, such as exposure room shielding, beam shutter, beam stopper, camera shielding, and collimator, are introduced in this research. These new instruments are made to upgrade the previous neutron radiography facility at RTP. Concrete mix design used in this study is based on the United Kingdom Department of Environment's design method

(DOE). The ferro-boron concrete samples are tested with several testing methods, including gamma radiation transmission testing, compressive strength testing (ASTM C109, 2016), rebound hammer testing, and ultrasonic velocity testing. Neutron and gamma profile at NUR-2 is determined by using two methods, namely simulation and experimental. Neutron and gamma profiles include flux and dose. Monte Carlo simulation code of MCNPX is used to simulate the parameters and instrument design of the neutron radiography components. TLD 600, TLD 700, and survey meter are used to measure the neutron and gamma doses around the facility. MICROSPEC-6 with neutron probe and gold foil are used to determine the neutron energy spectrum and neuron flux at the neutron beam respectively. A CCD camera and films are used to capture the neutron radiograph of the samples. In this research, direct exposure radiographic method is used because the sample is non-radioactive. Standard Image Quality Indicator (IQI) as per ASTM (ASTM E545, 2014) will be used to demonstrate the neutron radiography capability at the newly upgraded facility.

1.5 Significance of the Study

The significance of carrying out this research is that digital neutron radiography can be used as a complementary technique of other non-destructive types of testing such as X-ray and gamma radiography. Conventionally, neutron radiography used films to capture the radiograph. This method takes a lot of work and time to process the image. Hence, this research focusing on upgrading neutron radiography facility at RTP for digital neutron radiography using CCD camera. The newly upgraded facility also offers higher collimation ratio, which can be used for larger samples and produce better radiograph.

1.6 Structure of Thesis

This thesis details the work, results and analysis from the upgrading work of NR facility at the Reactor TRIGA PUSPATI. Generally, the content of this thesis is organized as follows:

Chapter 1 highlights a general introduction of NR, available facility in Malaysia and the importance of NR as complementary technique to conventional radiography. In addition, problem statement and objectives of this research are included in this chapter.

Chapter 2 contains the theoretical background of NR techniques. The performance of NR facilities from the other studies from around the world is presented. The procedure of NR applications and characterization of NR facility are discussed in the literature reviews included in this chapter.

Chapter 3 discusses the methodologies and materials used in this research. In this chapter, all materials used in fabrication of exposure room shielding, beam shutter, CCD camera shielding and in experiment done are discussed in detail. Furthermore, the methodology used in simulation, fabrication, experiment and characterization of the new NR facility are also discussed.

Chapter 4 presented the results and discussion of simulation and experimental work conducted in this research. The simulation and experiment of neutron and gamma profile from radial beam port 3 are defined. The discussion is extended further with the result of ferro boron concrete samples testing and characterization of the new NR facility at RTP. Lastly, Chapter 5 include the conclusions of this thesis and recommendations for future works.

REFERENCES

Akbay, İ., Köleli, D., Cömertpay, Ü., Güngör, A., & Özdemir, T. (2015). *Rubber for gamma and neutron radiation protection*.

Arno, M. (2009). Radiation Protection. In *Nuclear Engineering Handbook* (pp. 609-640): CRC Press.

Ashraf, M. M., & Khan, A. R. (1992). *Review of neutron radiographic applications in industrial and biological systems*. Retrieved from

American Society for Testing and Materials . *Standard Practice for Fabrication of Neutron Radiographic Sensitivity Indicators*. In. ASTM International, West Conshohocken, PA, E2023-10. 2014

American Society for Testing and Materials. *Standard Test Method for Determining Image Quality in Direct Thermal Neutron Radiographic Examination*. In. ASTM International, West Conshohocken, PA, E545. 2014

American Society for Testing and Materials. *Standard Practices for Thermal Neutron Radiography of Materials*. In. ASTM International, West Conshohocken, PA, E748-90. 2019

American Society for Testing and Materials. S*tandard Test Method for Compressive Strength of Hydraulic Cement Mortars (Using 2-in. or [50-mm] Cube Specimens)*. In. ASTM International, West Conshohocken, PA, C109 / C109M-16a. 2016

American Society for Testing and Materials. *Standard Test Method for Slump of Hydraulic-Cement Concrete*. In. ASTM International, West Conshohocken, PA, C143 / C143M – 12. 1999

American Society for Testing and Materials. *Standard Test Method for Determining the L/D Ratio of Neutron Radiography Beams*. In ASTM International, West Conshohocken, PA, E803-91. 2013

Anderson, I. S., McGreevy, R. L., & Bilheux, H. Z. (2009). *Neutron imaging and applications : a reference for the imaging community*. New York; London: Springer.

Azali Muhammad, Abdul Aziz Mohamed, Muhammad Rawi Mohamed Zin, Rafhayudi Jamro, Razali Kassim, Husain Wagiran, Hassan, W. M. S. W. (2008). Development of new neutron radiography facility at MINT TRIGA MARK II tangential beam port using CCD camera imaging system. *Neutron Imaging: A Non-Destructive Tool for Materials Testing*, 19-32.

Barton, J. P., & Rogers, J. D. (2015). Selective Energy Neutron Radiographic Imaging Origins and Lessons for Low Cost Systems. *Physics Procedia, 69*, 198-201. doi:http://dx.doi.org/10.1016/j.phpro.2015.07.028

Bastürk, M., Tatlisu, H., & Böck, H. (2006). Nondestructive inspection of fresh WWER-440 fuel assemblies. *Journal of Nuclear Materials, 350*(3), 240-245. doi:http://dx.doi.org/10.1016/j.jnucmat.2006.01.007

Berger, H. (1975). *Practical Applications of Neutron Radiography and Gaging. ASTM STP 586*: ASTM International, 1975.

Berger, H. (1965). *Neutron Radiography : Methods, Capabilities, And Applications* Elsevier Publishing Company.

Bossi, R. H., Iddings F.A., and Wheeler, G.C. (2002). *Nondestructive Testing Handbook* (Vol. Vol. 4): American Society for Nondestructive Testing, Inc., USA

Chalovich, T. R., Bennett, L. G. I., Lewis, W. J., & Brenizer Jr, J. S. (2004). Development of neutron radioscopy for the inspection of CF188 flight control surfaces. *Applied Radiation and Isotopes, 61*(4), 693-700. doi:http://dx.doi.org/10.1016/j.apradiso.2004.03.097

Craft, A. E., & Barton, J. P. (2017). Applications of Neutron Radiography for the Nuclear Power Industry. *Physics Procedia, 88*, 73-80. doi:https://doi.org/10.1016/j.phpro.2017.06.009

Davis, W. (2015). Procedures and Applications of Nondestructive Testing.

Dawson, M. N. (2008). *Applications of neutron radiography & tomography* (Doctoral dissertation, University of Leeds).

Demir, F., Budak, G., Sahin, R., Karabulut, A., Oltulu, M., & Un, A. (2011). Determination of radiation attenuation coefficients of heavyweight-and normal-weight concretes containing colemanite and barite for 0.663 MeV γ-rays. *Annals of Nuclear Energy, 38*(6), 1274-1278.

Domanus, J. C. (1992). Practical neutron radiography.

El-Khayatt, A. (2010). Radiation shielding of concretes containing different lime/silica ratios. *Annals of Nuclear Energy, 37*(7), 991-995.

Eldin, E. M. T. A. (2011). Neutron Radiography. *Thesis Master of Science in Nuclear Engineering*.

Grosse, M., Lehmann, E., Vontobel, P., & Steinbrueck, M. (2006). Quantitative determination of absorbed hydrogen in oxidised zircaloy by means of neutron radiography. *Nuclear Instruments and Methods in Physics Research Section A: Accelerators, Spectrometers, Detectors and Associated Equipment, 566*(2), 739-745. doi:http://dx.doi.org/10.1016/j.nima.2006.06.038

Hasham, R. (2008). *Parameters for Digital Neutron Radiography at TRIGA MARK II Research Reactor of Malaysia Nuclear Agency*. Universiti Teknologi Malaysia,

Harms, A. A., Blake, T. G., & Marton, J. P. (1973). Neutron imaging with thin gadolinium converters. *Nuclear Instruments and Methods, 109*(2), 253-255. doi:http://dx.doi.org/10.1016/0029-554X(73)90269-3

Hayashi, T., Tobita, K., Nakamori, Y., Orimo, S. (2009). Advanced neutron shielding material using zirconium borohydride and zirconium hydride. *Journal of Nuclear Materials, 386–388,* 119-121. doi:https://doi.org/10.1016/j.jnucmat.2008.12.073

Hilal, M. A., & Attallah, M. F. (2018). Investigation of chemical composition and moisture content for different materials on the attenuation of γ rays. *Radiochimica Acta, 106*(4), 337-344.

Idris, F. M. (1993). Neutron Flux Measurement of Reactor Triga Puspati (RTP). *User Manual for* RTP:1-5.

Jaafar, R. (1989). The Development of Neutron Radiography and Its Potential Application in Malaysia Industries, Neutron Radiography (3). *Proceedings of the Third World Conference, Osaka, Japan, May 14-18, 1989*.

Jamro, R., Kardjilov, N., HairieRabir, M., Zain, M. R. M., Mohamed, A. A., Ali, N. M., Mamat, M. R. (2017). Monte Carlo Simulation for Designing Collimator of the Neutron Radiography Facility in Malaysia. *Physics Procedia, 88*(Supplement C), 361-368. doi:https://doi.org/10.1016/j.phpro.2017.06.049

Keshavamurthy, R. S., Subramanian, D. V., Prasad, R. R., Haridas, A., Mohanakrishnan, P., & Chetal, S. C. (2011). Experimental Measurements of Neutron Attenuation in the Advanced Shield Material Ferro Boron in KAMINI Reactor. *Energy Procedia, 7*, 273-278. doi:http://dx.doi.org/10.1016/j.egypro.2011.06.035

Kok, K. D. (2009). *Nuclear Engineering Handbook*: CRC Press.

L'Annunziata, M. F. (2016). Chapter 1 - Radioactivity and Our Well-Being. In M. F. L'Annunziata (Ed.), *Radioactivity (Second Edition)* (pp. 1-66). Boston: Elsevier.

MacGillivray, G. (2011). Neutron Radiography Collimator Design. *Nray Services Inc., Petawa, Ontario, Canada*.

Martin, J. E. (2013). *Physics for radiation protection*. Weinheim: Wiley-VCH Verlag.

Muhammad Syahir,S ., Zainal, J., Jamro, R., Mohamed Zain, M. R., Mohamad Idris, F., Yazid, K. i., & Yassin, A. (2019). Beam characterization of new neutron radiography facility at TRIGA Mark II PUSPATI research reactor. *IOP Conference Series: Materials Science and Engineering, 555*, 012018. doi:10.1088/1757-899x/555/1/012018

Murray, R. L., & Holbert, K. E. (2015). Chapter 11 - Radiation protection*. In *Nuclear Energy (Seventh Edition)* (pp. 153-176). Boston: Butterworth-Heinemann.

Othman, M. b. (2012). *Monte carlo simulation of neutron radiography 2 (nur-2) system at triga mark ii research reactor of malaysian nuclear agency.* (Master of Science (Physics)),

Raad, M. J. A. d., & Kuiper, M. A. (2008). Industrial Radiography

Rabir, M. H., Abdul Karim, J., & Mohamed Zin, M. R. (2017). Neutron Flux Characterisation of Irradiation Facilities In Rtp. *Jurnal Sains Nuklear Malaysia*(2), 33-43%V 29.

Radiation Safety. (2012). (third edition ed.): Malaysian Nuclear Agency (Nuklear Malaysia).

Reijonen, H., Kormano, M., & Reijonen, K. (1973). Comparison of X-ray and Neutron Radiography of Pathologic Bone Samples. *Investigative Radiology, 8*(5), 326-332.

Resources, W. Properties of Ferro Boron. Retrieved from http://www.wbrl.co.uk/ferro-boron.html

Sarıyer, D., Küçer, R., Küçer, N. (2015a). Neutron Shielding Properties of Concrete and Ferro-Boron. *Acta Physica Polonica A, 128*(2B). doi:10.12693/APhysPolA.128.B-201

Sarıyer, D., Küçer, R., Küçer, N. (2015b). Neutron Shielding Properties of Concretes Containing Boron Carbide and Ferro – Boron. *Procedia - Social and Behavioral Sciences, 195*, 1752-1756. doi:http://dx.doi.org/10.1016/j.sbspro.2015.06.320

Solleh, M. R. M. (2015). *Moderator, Collimator And Shielding Studies For Bnct Research At Malaysian Nuclear Agency.* (Doctor of Philosophy), Universiti Sains Malaysia,

Strobl, M., Manke, I., Kardjilov, N., Hilger, A., Dawson, M., & Banhart, J. (2009). Advances in neutron radiography and tomography. *Journal of Physics D: Applied Physics, 42*(24), 243001.

LIST OF PUBLICATIONS

Indexed Conference Proceedings

1. **Muhammad Syahir**., et al. (2019). "Beam characterization of new neutron radiography facility at TRIGA Mark II PUSPATI research reactor." IOP Conference Series: Materials Science and Engineering **555**: 012018. **(Indexed by SCOPUS)**

2. **Muhammad Syahir,** S., et al. (2018). "Radiation shielding properties of ferro-boron concrete." IOP Conference Series: Materials Science and Engineering 298(1): 012037. **(Indexed by SCOPUS)**

APPENDICES

Appendix A MCNP Code Input Files for Simulation of the New Neutron Radiography Facility Instrumentations at RTP

1) New neutron radiography facility model at RTP

```
c   Exposure room
   1     1 -0.001183 1 2 -3 -4 5 -6 (-48 :4 :43 )(-1 :49 :42 )
   2     2   -2.3 1 2 -7 -8 9 -10 (4 :-5 :6 :3 :-2 :-1 )#8 #9 #200
   3     2   -2.3 1 2 -11 -12 13 -14 (8 :-9 :10 :7 :-2 :-1 )#8 #9 #300
   4     2   -2.3 1 2 -15 -16 17 -18 (12 :-13 :14 :11 :-2 :-1 )#7 #10 #400
   5     2   -2.3 1 2 -19 -20 21 -22 (16 :-17 :18 :15 :-2 :-1 )#7 #10
   6     1 -0.001183 1 2 -23 -24 25 -26 (20 :-21 :22 :19 :-2 :-1 )
c  Roof
   7     1 -0.001183 27 -28 29 -30 -19 11
   8     1 -0.001183 31 -32 33 -34 -11 3
c  Bunker door
   9     2   -2.3 2 -3 -5 13 35 -37
  10     2   -2.3 2 -39 -13 21 36 -38
c  Beam stopper
  11     1 -0.001183 -4 -43 48 #12 #13
  12     1 -0.001183 -44 47 -42 #13
  13     1 -0.001183 (-45 46 -41 ):(-46 48 -40 )
c  Beam shutter
  14     4   -1.19 -42 1 -51
  15     3  -11.35 -42 51 -50
  16    14    -3.2 -42 50 -49
c  Collimator
 101     6    -2.7 104 103 -102 -110
 102     6    -2.7 110 -1 111 -40
 103    10 -11.136 101 -103 104 -105
```

```
104     1 -0.001183 -101 104 -105
105     8      -4 101 -103 105 -106
106     1 -0.001183 -101 105 -106
108    10 -11.136 112 -103 -113 118
109     8      -4 113 107 -103 -114
110     1 -0.001183 113 -107 -114
111     8      -4 114 107 -103 -115
112     1 -0.001183 114 -107 -115
113    10 -11.136 115 107 -103 -110
114     1 -0.001183 115 -107 -110
115     6    -2.7 110 -111 -116 119
116     6    -2.7 116 -111 -117 120
117    10 -11.136 117 107 -111 -1
118     1 -0.001183 117 -107 -1
119     9  -9.747 112 -118 -113
120     1 -0.001183 110 -119 -116
121     1 -0.001183 116 -120 -117
122     7   -8.65 122 -103 -112 121
123     1 -0.001183 122 -121 -112
124     4  -0.941 106 -103 -124 123
125    11      -4 106 -123 -124
126     4  -0.941 124 -103 -122 126
127    11      -4 124 -126 -125
128     6    -2.7 125 -126 -122 121
129    11      -4 125 -121 -122
130    13   -3.35 127 -1 2 -23 21 -22 102 (-104 :110 :102 )(-110 :1 :40 )
131     1 -0.001183 127 -102 -104
999     0         (-1 :-2 :23 :24 :-25 :26 )(-127 :22 :-21 :1 :-2 :23 )
```

c Ferro boron stopper

```
200    12   -3.9 4 -8 -60
300    12   -3.9 8 -12 -60
400    12   -3.9 12 -16 -60

  1        px 0
```

2 pz -60
3 pz 60
4 px 220
5 py -75
6 py 75
c
7 pz 70
8 px 232.5
9 py -85
10 py 85
c
11 pz 80
12 px 245
13 py -95
14 py 95
c
15 pz 90
16 px 257.5
17 py -105
18 py 105
c
19 pz 100
20 px 270
21 py -115
22 py 115
c
23 pz 200
24 px 360
25 py -215
26 py 215
c
27 px 120
28 px 170
29 py -25

30 py 25

c

31 px 130

32 px 160

33 py -15

34 py 15

c

35 px 110

36 px 105

37 px 180

38 px 185

39 pz 65

c

40 cx 10

41 cx 12

42 cx 15

43 cx 20

44 px 215

45 px 205

46 px 202

47 px 200

48 px 195

49 px 50

50 px 20

51 px 10

60 sx 190 60

c collimator

101 kx -201 0.053300121670436 0

102 cx 7.5

103 cx 7.25

104 px -232

105 px -222

106 px -212

107 kx -285 0.00098761014501108 0

```
110     px -117
111     cx 9.75
112     px -204.38
113     px -189.38
114     px -179.38
115     px -169.38
116     px -115.8
117     px -114.6
118     cx 3
119     cx 5.3
120     cx 5.35
121     cx 1.5
122     px -204.48
123     cx 2.5
124     px -209.46
125     px -206.92
126     cx 2
127     px -250

mode  p
c     Air
m1    7014.     3.78621e-005
      8016.     1.01568e-005
c     Ordinary concrete
m2    1001.         0.00786
      8016.         0.0439 11023.         0.00105 12000.         0.00014
      13027.        0.00239 14000.        0.0158 19000.         0.00069
      20000.        0.00292 26000.        0.00031
c     Lead
m3    82000.50c         -1  $pb
c     Borated polyethylene
m4    1000.         -0.13653
      6000.         -0.81347 5000.         -0.05
c     SS-304
```

m5 24000. 0.01851242

25055. 0.001751896 28000. 0.006562605 26000. 0.06032172

c **Aluminium**

m6 13027. 0.06022142

c **Cadmium**

m7 48000. -1

c **Ferro boron**

m8 5011. -0.185

6012. -0.0032 13000. -0.0008 16000. -3e-005

14000. -0.0034 15031. -0.0003 26000. -0.80727

c **Bismuth**

m9 83209. -1

c **pb+4% antimony**

m10 82000.50c -0.96

51000.42c -0.04

c **Sapphire crystal**

m11 13027. 0.4

8016. 0.6

c **Concrete ferro boron**

m12 1001. -0.01326

6012. -0.0027704 8016. -0.344958 11023. -0.0091248

12000. -0.0007596 13027. -0.0122918 14000. -0.1841362

19000. -0.006027 20000. -0.0257706 26000. -0.326769

5011. -0.074 15031. -0.00012 16000. -1.2e-005

c **High density concrete**

m13 1001. 0.00786

8016. 0.0439 11023. 0.00105 12000. 0.00014

13027. 0.00239 14000. 0.0158 19000. 0.00069

20000. 0.00292 26000. 0.00031

c **Barite Colemanite Concrete**

m14 1001.70c -0.008564

5010.70c -0.009874 26054.70c -0.010378 20040.70c -0.085239

14028.70c -0.017733 12000.62c -0.097028 8016.70c -0.351537

56138.70c -0.410076 25055.70c -0.000101 16032.70c -0.097028

```
     13027.70c     -0.006146 11023.70c     -0.001108

imp:p   1024        2048 1r      4096 1r      8192        32          $ 1, 7
      16          2048        4096        1024 5r      1 3r        $ 8, 104
      2 1r        32          64 1r       128 1r       256 3r       $ 105, 116
      512 1r      32          256 1r      1 1r         4 1r         $ 117, 125
      16 3r       1 1r        0           2048 1r      4096         $ 126, 400
mt11 al27.12t
nps 100000000
c
sdef pos=-249.9 0 0 axs=1 0 0 ext=0 rad=d2 vec=1 0 0 dir=1 erg=d1 par=2
si1 l 1.00E-01 2.00E-01 3.00E-01 4.00E-01 5.00E-01 6.00E-01 7.00E-01 &
8.00e-01 9.00E-01 1.10E+00 1.20E+00 1.30E+00 1.40E+00 1.50E+00 &
1.60e+00 1.70E+00 1.80E+00 1.90E+00 2.10E+00 2.20E+00 2.30E+00 &
2.40e+00 2.50E+00 2.60E+00 2.70E+00 2.80E+00 2.90E+00 3.10E+00 &
3.20e+00 3.30E+00 3.40E+00 3.50E+00 3.60E+00 3.70E+00 3.80E+00 &
3.90e+00 4.10E+00 4.20E+00 4.30E+00 4.40E+00 4.50E+00 4.60E+00 &
4.70e+00 4.80E+00 4.90E+00 5.10E+00 5.20E+00 5.30E+00 5.40E+00 &
5.50e+00 5.60E+00 5.70E+00 5.80E+00 5.90E+00 6.10E+00 6.20E+00 &
6.30e+00 6.40E+00 6.50E+00 6.60E+00 6.70E+00 6.80E+00 6.90E+00 &
7.10e+00 7.20E+00 7.30E+00 7.40E+00 7.50E+00 7.60E+00 7.70E+00 &
7.80e+00 7.90E+00 8.10E+00 8.20E+00 8.30E+00 8.40E+00 8.50E+00 &
8.60e+00 8.70E+00 8.80E+00 8.90E+00 9.10E+00 9.30E+00 9.60E+00 &
9.70e+00 9.80E+00
sp1 0.26502 0.20326 0.09106 0.05187 0.03597 0.03245 0.02026 0.01671 &
0.01470 0.02486 0.00980 0.00951 0.00836 0.00792 0.00739 0.00724 &
0.00631 0.00574 0.01098 0.00616 0.07034 0.00235 0.00242 0.00361 &
0.00238 0.00214 0.00283 0.00850 0.00148 0.00143 0.00198 0.00324 &
0.00271 0.00190 0.00128 0.00300 0.00206 0.00313 0.00285 0.00076 &
0.00181 0.00079 0.00306 0.00304 0.00053 0.00409 0.00150 0.00045 &
0.00047 0.00130 0.00085 0.00031 0.00067 0.00044 0.00133 0.00141 &
0.00020 0.00079 0.00034 0.00021 0.00022 0.00056 0.00021 0.00040 &
0.00019 0.00056 0.00016 0.00017 0.00013 0.00484 0.01032 0.00016 &
0.00021 0.00004 0.00006 0.00008 0.00008 0.00021 0.00021 0.00030 &
```

```
0.00041 0.00039 0.00023 0.00012 0.00011 0.00005
si2 0 7.5
sp2 -21 1
c
e1 1.00E-01 2.00E-01 3.00E-01 4.00E-01 5.00E-01 6.00E-01 7.00E-01 &
8.00e-01 9.00E-01 1.10E+00 1.20E+00 1.30E+00 1.40E+00 1.50E+00 &
1.60e+00 1.70E+00 1.80E+00 1.90E+00 2.10E+00 2.20E+00 2.30E+00 &
2.40e+00 2.50E+00 2.60E+00 2.70E+00 2.80E+00 2.90E+00 3.10E+00 &
3.20e+00 3.30E+00 3.40E+00 3.50E+00 3.60E+00 3.70E+00 3.80E+00 &
3.90e+00 4.10E+00 4.20E+00 4.30E+00 4.40E+00 4.50E+00 4.60E+00 &
4.70e+00 4.80E+00 4.90E+00 5.10E+00 5.20E+00 5.30E+00 5.40E+00 &
5.50e+00 5.60E+00 5.70E+00 5.80E+00 5.90E+00 6.10E+00 6.20E+00 &
6.30e+00 6.40E+00 6.50E+00 6.60E+00 6.70E+00 6.80E+00 6.90E+00 &
7.10e+00 7.20E+00 7.30E+00 7.40E+00 7.50E+00 7.60E+00 7.70E+00 &
7.80e+00 7.90E+00 8.10E+00 8.20E+00 8.30E+00 8.40E+00 8.50E+00 &
8.60e+00 8.70E+00 8.80E+00 8.90E+00 9.10E+00 9.30E+00 9.60E+00 &
9.70e+00 9.80E+00
f1:p 104 105 106 124 125 112 113 114 115 110 1
c
tmesh
 rmesh11:p dose 10 1 2 1
  cora11  0 71i 360
  corb11  -215 85i 215
  corc11  -25 25
 rmesh21:p dose 10 1 2 1
  cora21  0 71i 360
  corb21  -25 25
  corc21  -60 51i 200
 rmesh41:p dose 10 1 2 1
  cora41  -232 231i 0
  corb41  -10 19i 10
  corc41  -0.5 0.5
endmd
```

2) Ferro boron concrete

```
   1     2      -4 -1  u=1
   2     1    -2.3 1  u=1
  20     1    -2.3 -20  fill=1 u=11 lat=1
c
  30     1    -2.3 22 -23 24 -25 26 -30  fill=11
  31     1    -2.3 22 -23 24 -25 30 -31  fill=11
  32     1    -2.3 22 -23 24 -25 31 -32  fill=11
  33     1    -2.3 22 -23 24 -25 32 -33  fill=11
  34     1    -2.3 22 -23 24 -25 33 -34  fill=11
  35     1    -2.3 22 -23 24 -25 34 -35  fill=11
  36     1    -2.3 22 -23 24 -25 35 -36  fill=11
  37     1    -2.3 22 -23 24 -25 36 -37  fill=11
  38     1    -2.3 22 -23 24 -25 37 -38  fill=11
  39     1    -2.3 22 -23 24 -25 38 -27  fill=11
c
  90     0         22 -23 24 -25 28 -26
 100     0         -22 :23 :-24 :25 :-28 :27

   1       rpp -1.5 1.5 -1.5 1.5 -1.5 1.5
c
  20       rpp -3.232 3.232 -3.232 3.232 -3.232 3.232
c
  22        pz -50
  23        pz 50
  24        py -50
  25        py 50
  26        px -50
c
  30        px -40
  31        px -30
  32        px -20
  33        px -10
```

```
  34       px 0
  35       px 10
  36       px 20
  37       px 30
  38       px 40
c
  27       px 50
  28       px -60

mode  n
m1    1001.          -0.01
     6012.          -0.001 8016.        -0.529107 11023.          -0.016
     12000.          -0.002 13027.       -0.033872 14000.        -0.337021
     19000.          -0.013 20000.          -0.044 26000.          -0.014
m2    5011.          -0.185
     6012.          -0.0032 13000.         -0.0008 16000.         -3e-005
     14000.         -0.0034 15031.         -0.0003 26000.        -0.80727
imp:n   1 3r        4           8           16          32           $ 1, 34
      64          128         256         512         1024         $ 35, 39
      1           0           $ 90, 100
nps 100000000
sdef pos=0 0 0 axs=1 0 0 ext=0 x=-60 y=d1 z=d2 vec=1 0 0 dir=1 erg=d3 par=1
si1 -50 50
sp1 0 1
si2 -50 50
sp2 0 1
si3 l 2.5e-8 4.0e-7
sp3 0.5 0.5
f2:n 26 30 31 32 33 34 35 36 37 38 27
f4:n 90 30 31 32 33 34 35 36 37 38 39
f12:n 26 30 31 32 33 34 35 36 37 38 27
df12 ic=10 iu=2 fac=1
f14:n 90 30 31 32 33 34 35 36 37 38 39
df14 ic=10 iu=2 fac=1
```

3) Beam Shutter

```
MCNPX Visual Editor Version X_24E
c     Created on: Tuesday, January 09, 2018 at 09:38
  10     1   -0.95 2 -3 7 -6 8 -9
  20     3  -11.34 3 -4 7 -6 8 -9
  30     4    -3.2 4 -5 7 -6 8 -9
  50     5   -7.85 6 -11 2 -5 -9 8
  60     5   -7.85 12 -7 2 -5 -9 8
  70     5   -7.85 10 -8 2 -5 12 -11
  40     0         #10 #20 #30 #50 #60 #70 -1
  99     0         1

   1        so 1000
   2        px 0
   3        px 10
   4        px 25
   5        px 50
   6        py 20
   7        py -20
   8        pz -20
   9        pz 20
  10        pz -21
  11        py 21
  12        py -21

mode  n
m1    5010.66c         0.0098  $5% Borated Polyethylene
     5011.66c         0.0402 6012.42c         0.8132 1001.66c         0.1368
m2    5010.66c          0.049  $30% Borated Polyethylene
     5011.66c          0.201 6012.42c         0.8132 1001.66c         0.1368
m3    82207.66c             1  $lead
m4    1001.66c       0.008564  $Barite-colemanite concrete
     5010.66c       0.009874 12000.66c      0.097028 16032.66c      0.097028
```

```
     26056.66c      0.010378 80000.42c      0.351537 13027.66c      0.006146
     20040.21c      0.085239 56138.66c      0.410076 11023.66c      0.001108
     14028.66c      0.017733 25055.66c      0.000101
m5    6000.70c          0.16  $Mild Steel
     14000.60c          0.4 25055.70c          0.7 16000.62c          0.04
     15031.70c          0.04
imp:n   4           8           16          1 3r        0           $ 10, 99
nps 100000000
sdef pos=0 0 0 axs=1 0 0 ext=0 x=0 y=d1 z=d2 vec=1 0 0 dir=1 erg=d3 par=1
si1 -20 20
sp1 0 1
si2 -20 20
sp2 0 1
si3 l 1.00E-10 1.26E-10 1.58E-10 2.00E-10 2.51E-10 3.16E-10 3.98E-10 &
5.01e-10 6.31E-10 7.94E-10 1.00E-09 1.26E-09 1.58E-09 2.00E-09 &
2.51e-09 3.16E-09 3.98E-09 5.01E-09 6.31E-09 7.94E-09 1.00E-08 &
1.26e-08 1.58E-08 2.00E-08 2.51E-08 3.16E-08 3.98E-08 5.01E-08 &
6.31e-08 7.94E-08 1.00E-07 1.26E-07 1.58E-07 2.00E-07 2.51E-07 &
3.16e-07 3.98E-07 5.01E-07 6.31E-07 7.94E-07 1.00E-06 1.26E-06 &
1.58e-06 2.00E-06 2.51E-06 3.16E-06 3.98E-06 5.01E-06 6.31E-06 &
7.94e-06 1.00E-05 1.26E-05 1.58E-05 2.00E-05 2.51E-05 3.16E-05 &
3.98e-05 5.01E-05 6.31E-05 7.94E-05 1.00E-04 1.26E-04 1.58E-04 &
2.00e-04 2.51E-04 3.16E-04 3.98E-04 5.01E-04 6.31E-04 7.94E-04 &
1.00e-03 1.26E-03 1.58E-03 2.00E-03 2.51E-03 3.16E-03 3.98E-03 &
5.01e-03 6.31E-03 7.94E-03 1.00E-02 1.26E-02 1.58E-02 2.00E-02 &
2.51e-02 3.16E-02 3.98E-02 5.01E-02 6.31E-02 7.94E-02 1.00E-01 &
1.26e-01 1.58E-01 2.00E-01 2.51E-01 3.16E-01 3.98E-01 5.01E-01 &
6.31e-01 7.94E-01 1.00E+00 1.26E+00 1.58E+00 2.00E+00 2.51E+00 &
3.16e+00 3.98E+00 5.01E+00 6.31E+00 7.94E+00 1.00E+01
sp3 0.00001 0.00001 0.00001 0.00002 0.00002 0.00002 0.00005 0.00007 &
0.00010 0.00015 0.00027 0.00041 0.00063 0.00077 0.00107 0.00178 &
0.00302 0.00450 0.00618 0.00936 0.01397 0.02147 0.03026 0.03898 &
0.05145 0.06888 0.08218 0.09226 0.09555 0.08646 0.06938 0.04847 &
0.02816 0.01498 0.00747 0.00484 0.00419 0.00371 0.00342 0.00329 &
```

```
0.00316 0.00311 0.00302 0.00305 0.00287 0.00284 0.00287 0.00278 &
0.00274 0.00278 0.00279 0.00269 0.00277 0.00282 0.00265 0.00267 &
0.00270 0.00279 0.00269 0.00282 0.00276 0.00269 0.00278 0.00263 &
0.00267 0.00264 0.00265 0.00266 0.00263 0.00262 0.00266 0.00272 &
0.00268 0.00273 0.00267 0.00271 0.00271 0.00285 0.00262 0.00258 &
0.00263 0.00272 0.00268 0.00275 0.00297 0.00390 0.00173 0.00245 &
0.00284 0.00376 0.00195 0.00297 0.00325 0.00286 0.00287 0.00344 &
0.00370 0.00347 0.00383 0.00436 0.00445 0.00470 0.00486 0.00466 &
0.00380 0.00247 0.00141 0.00208 0.00147 0.00074 0.00018
tmesh
 rmesh11:n dose 10 1 2 1
  cora11  0 5i 60
  corb11  -20 3i 20
  corc11  -20 20
 rmesh21:n dose 10 1 2 1
  cora21  0 5i 60
  corb21  -20 20
  corc21  -20 3i 20
endmd
```

Appendix B (DOE) Method Form

BS - CONCRETE MIX DESIGN (DOE)

DOE METHOD OF CONCRETE MIX DESIGN: The British method of concrete mix design, popularly referred to as the "DOE method", is used in the United Kingdom and other parts of the world and has a long established record. The method originates from the "Road Note No 4" which was published in Great Britain in 1950. In 1975 the note was replaced by the "Design of Normal Concrete Mixes", published by the British Department of the Environment (DOE). In 1988 the "Design of Normal Concrete Mixes" was issued in a revised and updated edition to allow for changes in various British Standards.

DOE mix design generally involves the following stages.

1. Determine the target strength
2. Determine the water/cement (W/C) ratio according to the target strength, types of cement and aggregate.
3. Determine the water content, W, from required workability, size and type of aggregate.
4. Determine cement content, C, from W/C ratio and water content.
5. Estimate the density of wet fresh concrete, D, based on relative density of combined aggregate and water content.
6. Determine the total aggregate content from D, C, and W.
7. Determine the proportion of fine aggregate according to the fineness of fine aggregate, maximum aggregate size, slump/Vebe time and W/C.
8. Determine coarse aggregate.

Specified Strength and Target Strength For Mix Design

a. Variation and probability of concrete strength finding standard deviation and k values to calculate the margin.

b. Characteristic strength Probability and statistics have been widely adopted in engineering to describe structure failure and material properties. In the old practice, concrete strength is specified using "minimum strength". From the probability theory adopted today, there is always a possibility, however remote, that the strength of concrete falls below a specified strength. Therefore concrete strength is specified in term of "Characteristic Strength". The characteristic strength is the strength below **2** which a specified proportion of test results, often called "defectives", may be expected to fall. The characteristic strength may be defined to have any proportion of defectives, BS 5328 "Concrete" and BS8110 "Structure use of concrete" adopt 5% defectives level for the determination of characteristic strength.

c. **Target strength for mix design**
As a results of variability of concrete it is necessary to design the mix to have a mean strength greater than the specified characteristic strength by an amount termed the **margin**. Thus the **target strength**, fm, is

fm= fc+ ks ……..(3)
where
fc= specified characteristic strength
s = standard deviation
k = constant depending on the defective level associated with the specified strength. ks is termed the margin.

Normal Distribution

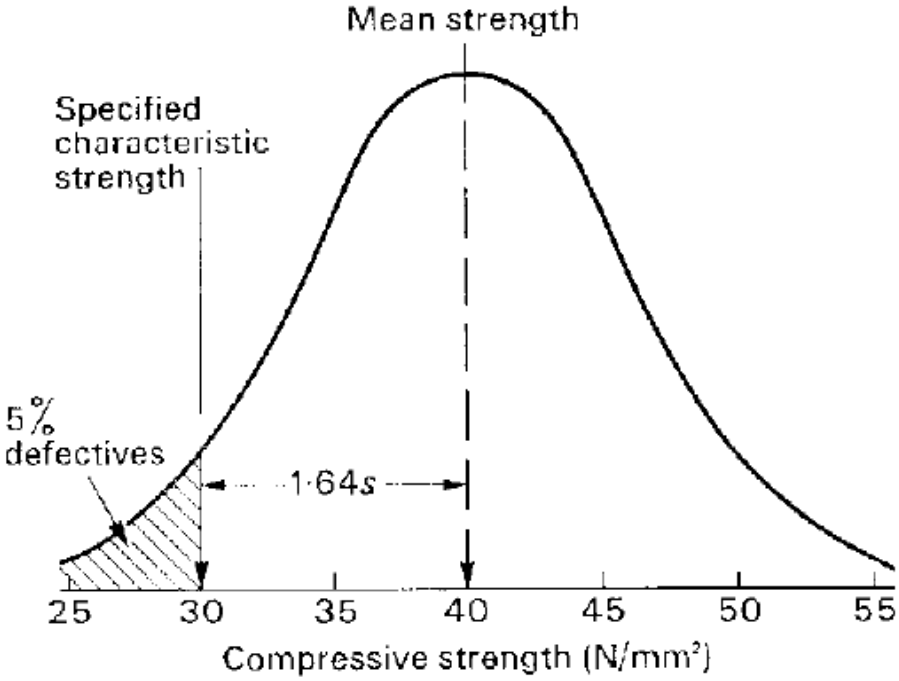

Mean = failure level+ z x standard deviation.

A table of z (or n) values for various values of percentage failures **3**

(Table 1.10.1 in section 1.10 of the notes)

Percentage failure permitted	Z value
16	1.00
10	1.28
5	1.64
2.5	1.96
2	2.05
1	2.33

Figure 3

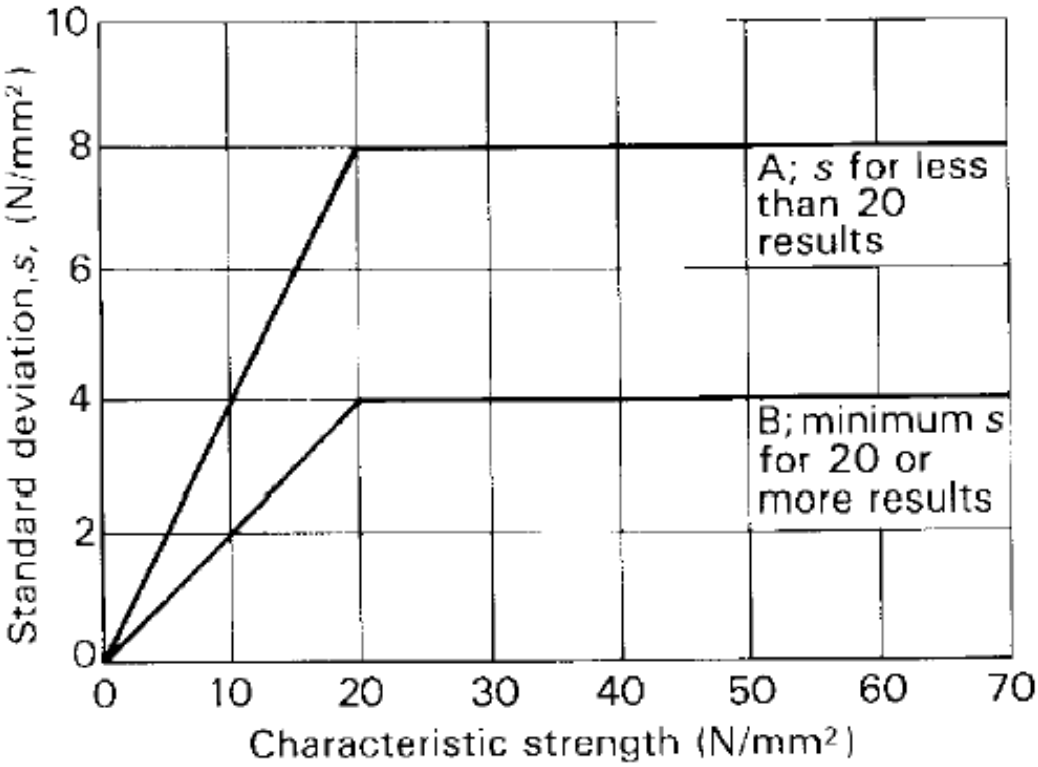

- **Find w/c by:**

1. Finding strength from table 2 (with w/c =0.5)
2. Using this strength with w/c 0.5 to drew a curve parallel to other curves in the figure 4
3. Intersection of the line that represent target strength with this curve will determine w/c

Table 2 Compressive strength of concrete made with w/c 0.5 as per 1988 British Method

S. No.	*Type of cement*	*Type of coarse aggregate C.A.*	*Compressive cube strength at the age in MPa*			
			3 days	7 days	28 days	91 days
1.	Ordinary portland cement (type I)	Un crushed	18 — 22	27 — 30	40 — 42	48 — 49
2.	Sulphate resisting cement (type V)	Crushed	23 — 27	33 — 36	47 — 49	55 — 56
3.	Rapid hardening portland cement (type III)	Un crushed crushed	25 — 29 30 — 34	34 — 37 40 — 43	46 — 48 53 — 55	53 — 54 60 — 61

Note. Higher value may be adopted

Figure 4

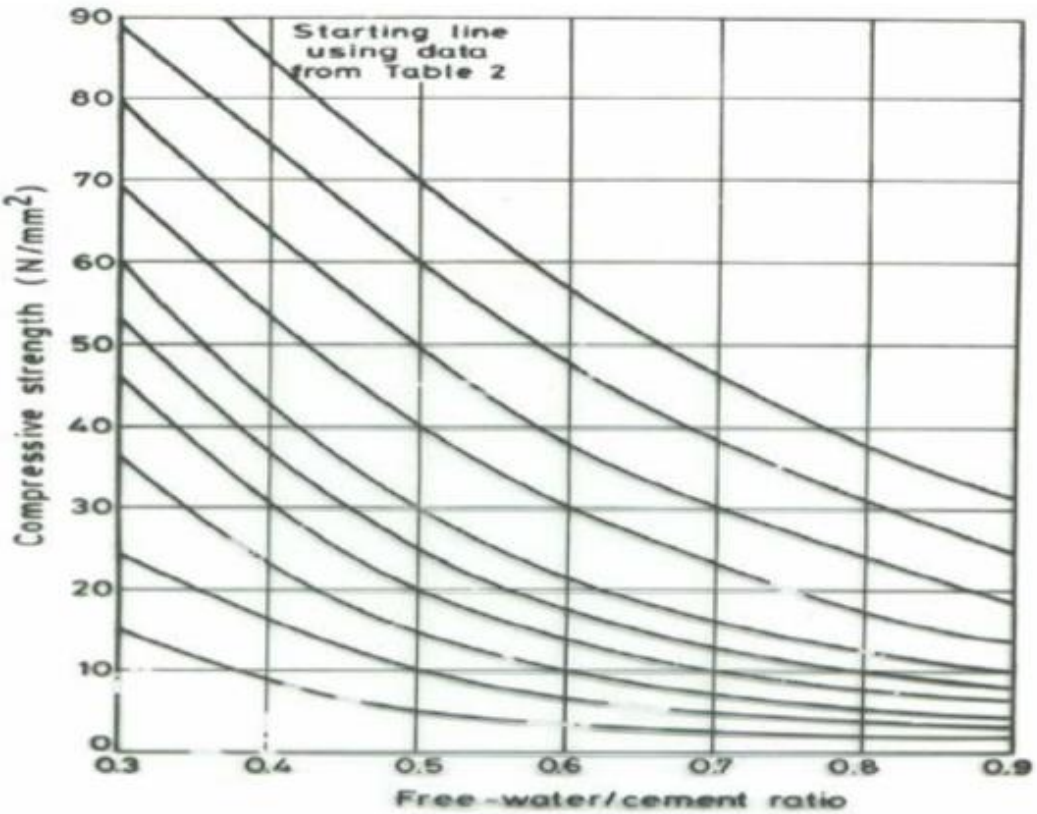

Table 3 Approx water contents (kg/m^3) required to give workability					
Slump (mm)		0-10	10-30	30-60	60-180
Vebe time (s)		more than 12	6-12	3-6	0-3
Maximum aggregate size (mm)	Type of aggregate				
10	Uncrushed	150	180	205	225
	Crushed	180	205	230	250
20	Uncrushed	135	160	180	195
	Crushed	170	190	210	225
40	Uncrushed	115	140	160	175
	Crushed	155	175	190	205

• Calculate total Aggregate content

• Total aggregate content = Wet density-C-W

• C: cement content Kg/m3

• W:water content Kg/m3

• Wet density from figure 5 depending on specific weight of aggregate and water content

Figure 5

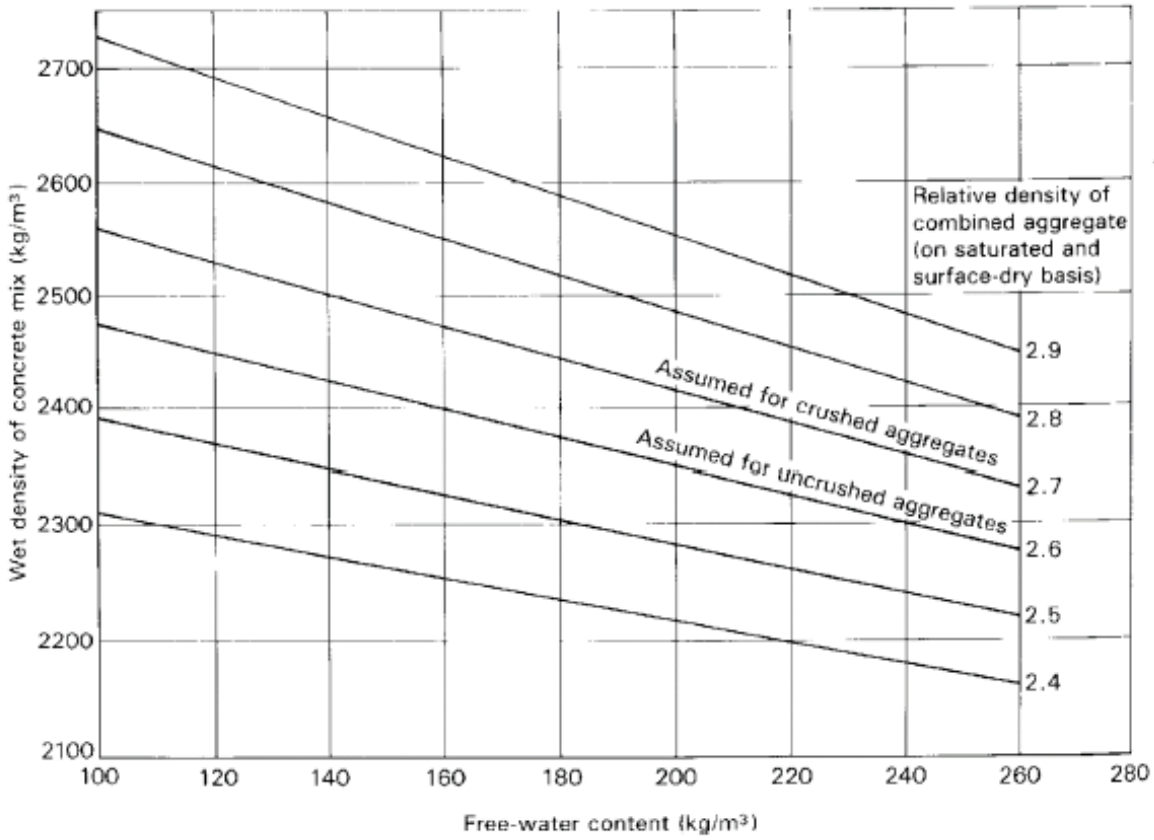

To find the percent of fine aggregate

• Using figure 6 to find the percent of fine aggregate through knowing :

1. Slump and V-B time
2. Max aggregate size
3. Water to cement ratio w/c
4. By knowing the zone of grading for the aggregate, 2 values would be obtained (take the average)

Figure 6 (10mm)

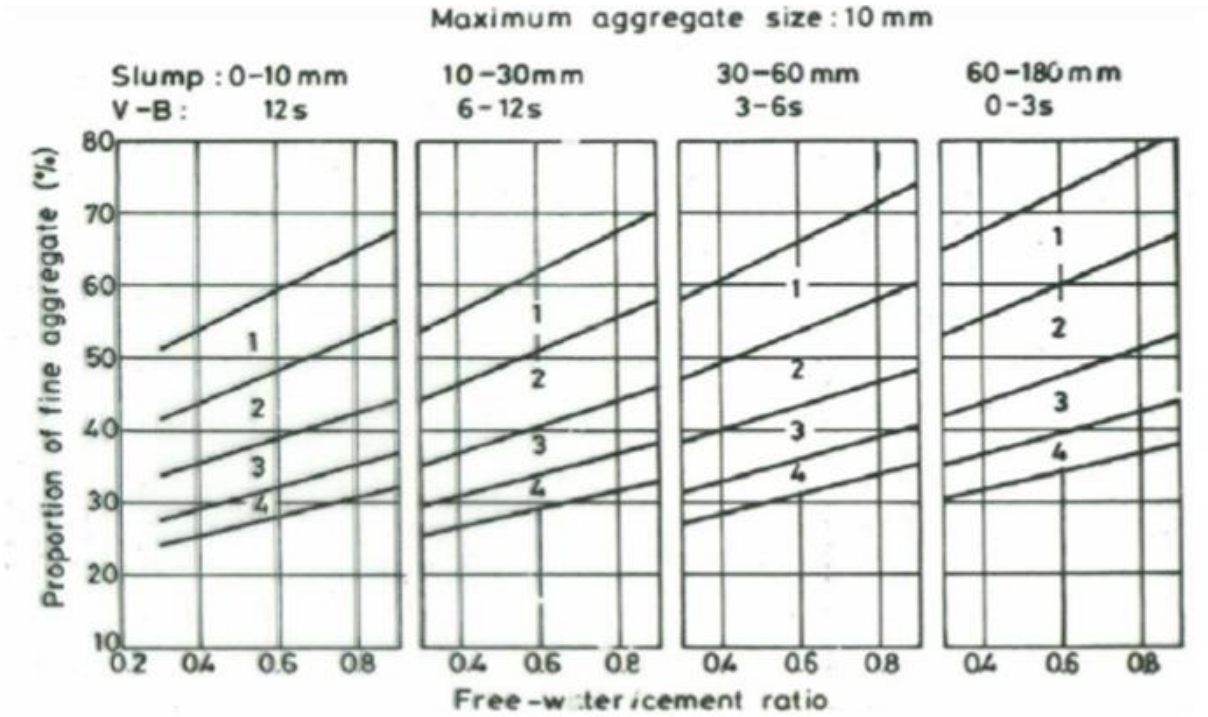

Figure 6 (20mm)

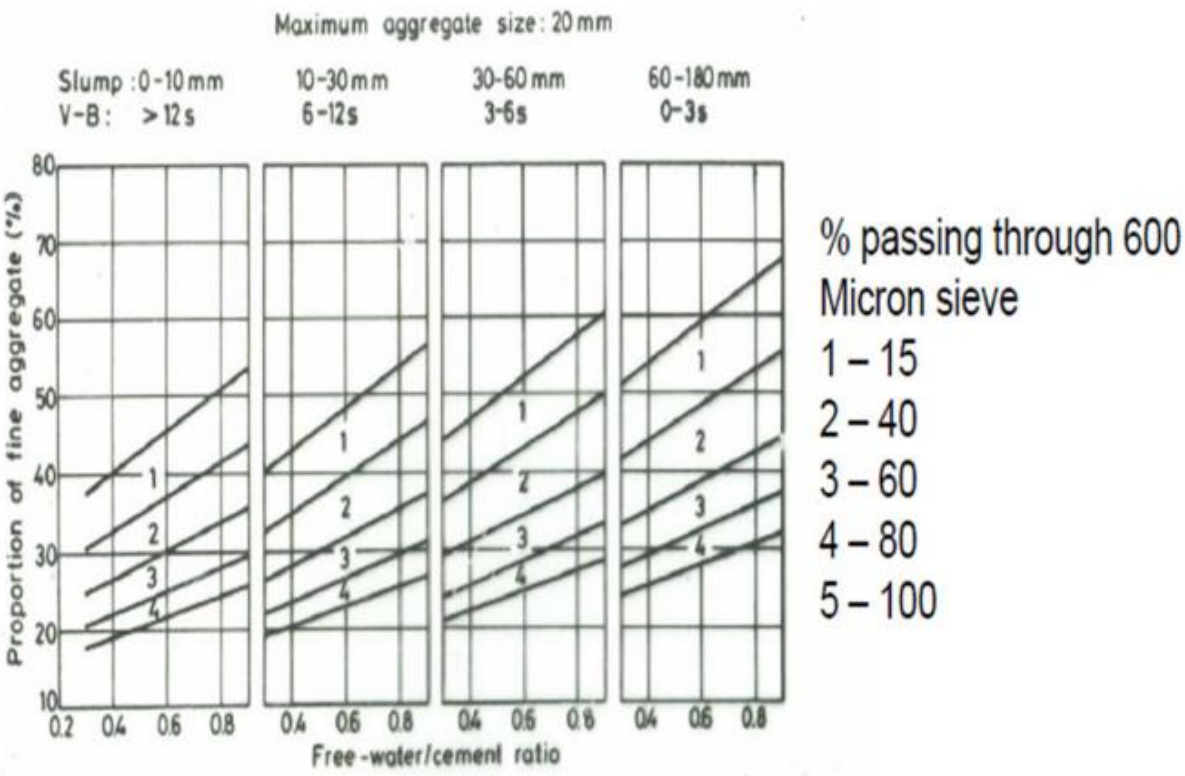

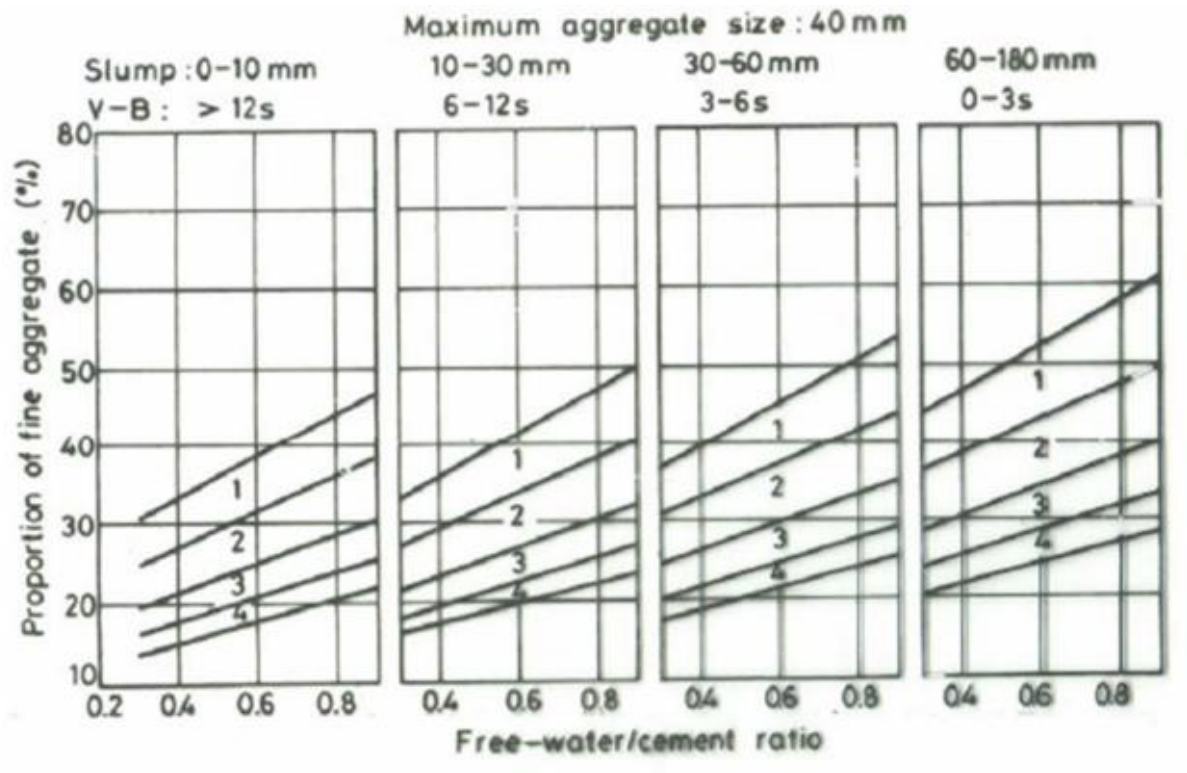

• Calculate Fine Aggregate content

• Fine aggregate content Fagg = pw×(Wagg) kg/m3

• Pw (percent of fine agg.) is determined from graphs

• Cagg= Wagg-Fagg

Material	**Content (Kg/m^3)**
water	
Cement	
Fine aggregate	
Coarse aggregate	
Density	
w/c	
Mix proportions (cement:sand:gravel)	**X:Y:Z**

Appendix C Film Processing

Darkroom safe lighting

X-ray films and paper can be handled under the normal orange-red or green darkroom safelights for X-ray films. When doing so care must, of course, be taken to see that the distance from the safelight and the duration of exposure are appropriate to the speed of the film concerned. Recommended safelight filters: R 1 (orange -red) and G 7 (green).

Developing

Standardised development is essential if exact exposure data are to be found by experiment and then applied systematically, the use of a standard developer at a standard temperature, with standard developing times. Standard developer: i.e. developer of uniform, constant characteristics (composition). Preferably use G 127 developer; this will obviate variations in density due to incorrect mixing of the bath or the use of impure chemicals. Standard developing times: the times advised will give the best results. Altering the developing time to suit the exposure is not to be recommended. Standard temperature: 68°F (20°C), in no circumstances below 64"F (18°C).

Developer temperature

Increasing the temperature of the developer speeds up the developing process. This cuts down the developing time, but the developer then becomes exhausted more rapidly, and faults aggravated by the age of the film or too exhausted or oxidized processing solutions can very readily occur. Conversely, the activity of the developer is reduced when its temperature drops. Developing times for temperature other than the recommended one of 68°F (20°C) are given here in case it should not be possible to bring the developer to this temperature and keep it there during development.

Developing times (in minutes) for tank development in the conventional X-ray developers (e.g.

G 127), at different temperatures.

Structurix film	*64°F 18°C*	*68°F 20°C*	*72°F 22°C*	*75°F 24°C*	*79°C 26°C*	*82°F 28°C*	*86°F 30°C*
D 2							
D 4							
D 5	*6*	*5*	*4*	*3.5*	*3*	*2.5*	*2*
D 7							
D 10							

Agitation of films

The film should be agitated continuously for the first 30 seconds of development, in order to dislodge any air-bubbles which may have formed on the surface of the emulsion (and which would cause white spots on the radiograph), and to distribute the developer evenly to all areas of the emulsion. If agitation is continuous the development process will be speeded up, and the

times given here can then be cut by about l/5th.

When using frames with clips, never let the films drain above the developer tank; immerse them immediately in the stop bath or rinse. About 320 ml of developer is carried over by the film (and frame) for every square metre of film processed. Since, for every square metre of film developed, 600 ml of developer lies to be replaced by a similar amount of replenishes, this means that a further 280 ml of developer will need to be removed from the tank later. When using frames with channels, allow the film to drain over the developer tank for two or three seconds. In this way, about 400 ml of developer will be carried over for each square metre of film processed. It follows that a quantity of 200 ml should be drained from the tank in order to add 600 ml of replenishes.

Replenishment

Replenisher can be added up to maximum of 4 litres to every litre of original developer solution. After adding the last dose of replenisher, a quarter of a square metre of film can be processed per litre of solution before the developer bath needs to be discarded and replaced.

Stop bath

It is preferable to immerse the film for 30 seconds, immediately after removal from the developer, in a stop bath in order to prevent, 1) neutralisation of the fixer by the transfer of

alkaline developer on the films and hangers; 2) streaks or dichroic fog on the films. The stop bath must be kept at a sufficient level of acidity. If a stop bath is not used, films should be rinsed in running water for 2-3 minutes immediately after development.

Fixing

The following fixers are recommended:

1) non-hardening fixer G 321

2) hardening fixers:

a) formula GP 308

b) G 321 with the addition of Aditan hardener.

Films should be fixed for double the time taken for cleaning the emulsion (disappearance of

the opalescent milkiness).

As a general rule, not more than one square metre of film can be processed per litre of fixer. Films must be agitated continuously during the first 30 seconds of fixing, particularly when a hardening fixer is involved; failure to do this can result in a deposit forming in the fixer which appears as white patches on the film. This deposit can be removed by placing the films in a 10% solution of sodium carbonate. An over-warm processing bath has a tendency to strip the emulsion from its base and to melt the emulsion (see Washing, below). For this reason, a hardening fixer should be used wherever the temperature of the washing water is higher than 7TF (25"C).

Final wash

Thee silver compounds which are formed during the fixing stage must be removed from the emulsion, since they can affect the silver image at the later stage. For this

reason the film must be washed thoroughly in running water. The duration of washing will depend upon the temperature of the water used:

at 41 - 54°F (5 - ITC) wash for 30 min.,

at 55 - 7TF (13 - 25°C) wash for 20 min.,

at 78 - 86°F (26 - 30°C) wash for 15 min.,

at more than 86°F (30°C) wash for 10 min.

Avoid temperatures above 77°F (25e'C) if possible.

Draining

Leave films to drain for 2 minutes or so before placing them in the drying cabinet; this will keep the floor of the cabinet dry. It is advisable to immerse films for 1 minute in a solution of wetting agent after the final wash. The films then will drain more quickly, completely and evenly, and as no droplets of water will be left on the surface of the films there will be less risk of drying marks.

Drying

X-ray films should preferably be dried in a specially-designed drying cabinet; if not, they must be dried in a dry, dust-free room. The higher the temperature and the lower the relative humidity, the more rapidly the film will dry; temperatures higher than 104°F (40°C) must however be avoided, as they will involve the risk of melting the gelatine or stripping the emulsion from its base. The flow of air reaching the films must be even; excessively forced ventilation, producing an uneven flow of air inside the drying cabinet, can cause abnormal curling or distortion of the films. Practical advice on avoiding processing faults will be found in the booklet "50 Hints on the darkroom processing of industrial X-ray films", produced specially for darkroom staff.

Source: Domanus, J. C. (1992). Practical neutron radiography.

Appendix D Thermal Neutron Flux Measurement Using Gold and Cadmium

The neutron energy range can roughly be categorized into three groups, each with its own characteristics. Table 3.8 lists the three main neutron groups.

Table 1 Three main neutron groups

Group	Energy range	Region
Fast	10 keV – 10 MeV	Fission
Resonance	1 eV – 10 keV	1/E
Thermal	0 - eV	Maxwellian

with E as the neutron's energy

For gold (Au), its response region is in between 0.0014 eV to 5.8 eV, which can only absorb thermal and epithermal neutrons. If the cut-off energy of cadmium (Cd) i.e. 0.55 eV is used to mark the thermal and epithermal regions, the difference between the activity of bare gold wire and the gold wire covered with cadmium can be determined. If both were irradiated in the same flux under the same circumstances, the activity caused by thermal neutron flux can be determined (Idris, 1993). The activity of bare gold wire induced by neutrons is given by:

$$\mathrm{A_{bare}}(\tau) = \Phi_{\mathrm{th}}\sigma_{\mathrm{th}}\mathrm{N_s}(1-\exp(-\lambda t))\exp(-\lambda\tau) + \Phi_{\mathrm{epi}}\sigma_{\mathrm{epi}}(1-\exp(-\lambda t))\exp(-\lambda\tau) \quad (1)$$

The activity of gold wire covered with 1 mm cadmium is given by:

$$\mathrm{A_{Cd}}(\tau) = \Phi_{\mathrm{epi}}\sigma_{\mathrm{epi}}\mathrm{N_s}(1-\exp(-\lambda t))\exp(-\lambda\tau) \quad (2)$$

with

σ_{th} Thermal neutron cross section, with value 98.8 barn

σ_{epi} Epithermal cross section

Φ_{th} Thermal flux

Φ_{epi} Epithermal flux

As $A_{thermal} = A_{bare}(\tau) - A_{Cd}(\tau)$, therefor the difference (1)-(2) will give:

$$A_{thermal}(\tau) = \Phi_{th}\sigma_{th}N_s(1 - \exp(-\lambda t))\exp(-\lambda\tau) \quad (3)$$

From equation (3.6), the thermal neutron flux $\emptyset_{th}$ can be calculated.

For epithermal neutron of a gold detector, its resonance integral is given by:

$$I_r = \int_{0.55\ eV}^{0.2\ MeV} \sigma(E)\,\frac{dE}{E} = 1562\ barn \quad (4)$$

Therefore, its reaction rate with epithermal neutron is given by:

$$R = \theta \int_{0.55\ eV}^{0.2\ MeV} \sigma(E)\frac{dE}{E} \quad (5)$$

$$= \theta\, I_r$$

$$= \theta\, 1562\ barn$$

with θ as the intermediate neutron flux density per unit 'lethargy' and has a constant value. The cadmium ratio is defined as

$$R_{Cd} = \frac{A_{bare}}{A_{Cd}} \quad (6)$$

$$= \frac{A_{th} + A_{epi}}{A_{th}}$$

$$= 1 + \frac{A_{epi}}{A_{th}}$$

or,

$$R_{Cd} - 1 \approx \frac{r_{th}}{r_{epi}} \quad (7)$$

and

$$R_{Cd} = \frac{\Phi_{th}\sigma_{th} + \Phi_{th}\sigma_{epi}}{\Phi_{epi}\sigma_{epi}} \quad (8)$$

Thus, the ratio of a bare gold detector and the one covered with Cd could be written as:

$$R_{Cd} - 1 \approx \frac{\Phi_{th}\sigma_{th}}{\theta \int_{0.55\ eV}^{0.2\ MeV} \Phi_{epi}(E)\frac{dE}{E}} \quad (9)$$

$$\approx \frac{\Phi_{th}\sigma_{th}}{\theta\, 1562\ barn}$$

From equation (3.12), the value of θ could be calculated. Therefore, the total intermediate neutron flux detected by gold is:

$$\Phi_{\mathrm{int}} = \theta \int_{0.55\ \mathrm{eV}}^{0.2\ \mathrm{MeV}} \Phi_{\mathrm{epi}}(\mathrm{E}) \frac{\mathrm{dE}}{\mathrm{E}} \approx \theta \ln \frac{0.2\ \mathrm{E} + 06}{0.5} \tag{10}$$

Pre-Irradiation calculations

Before the irradiation of the samples was carried out using the reactor, it was important to calculate the activity of the samples prior irradiation for safety purposes. The expected activity of each material was estimated using the equation below:

$$\mathrm{A_s} = \mathrm{N_t}\sigma\Phi(1 - \exp(-\lambda \mathrm{t}))\exp\,(-\lambda\tau) \tag{11}$$

with,

Φ	neutron flux at measurement point
σ	neutron cross section of the target nuclide
N_t	total number of target nuclides in the sample
λ	decay constant

A neutron flux of $1x10^6$ $n.cm^{-2}.s^{-1}$ was used for the pre-irradiation calculations (Hasham, 2008).